JOURNAL OF CATALYSIS **174,** 210–218 (1998)
ARTICLE NO. CA981971

On the Regeneration of Coked H-ZSM-5 Catalysts

Sung-Jeng Jong,* Ajit R. Pradhan,* Jin-Fu Wu,* Tseng-Chang Tsai,† and Shang-Bin Liu*,[1]

*Institute of Atomic and Molecular Sciences, Academia Sinica, P.O. Box 23-166, Taipei, Taiwan 10764, Republic of China; and †Refining and Manufacturing Research Center, Chinese Petroleum Corporation, Chiayi, Taiwan 60038, Republic of China
E-mail: sbliu@sinica.edu.tw

Received August 4, 1997; revised November 17, 1997; accepted November 18, 1997

Regeneration of H-ZSM-5 zeolite coked during ethylbenzene conversion is studied. Selective removal and transformation of the carbonaceous compounds during reactivation in the presence of air, 0.5% O_2 in N_2 and H_2 at 500°C were examined using the combination of GC, TGA, xenon adsorption, IR, ^{129}Xe, and ^{13}C CP-MAS NMR spectroscopy and ethylbenzene transformation as a test reaction. A rapid initial rate of regeneration is found while the fouled catalysts were subjected to regeneration in air. The intracrystalline cokes present near the Brønsted acid sites are preferentially removed to those present on the external surface of the zeolite crystallites. The phenomenon is more obvious when using H_2 as the regenerating gas. During the oxidative removal of the coke with air or 0.5% O_2 in N_2, a portion of the carbonaceous compounds was transformed to more condensed structures before getting completely oxidized. In the presence of H_2, while the internal cokes were selectively removed by hydrocracking, the external cokes were partially cracked from bulky alkyl polyaromatic compounds to less bulky polyaromatic compounds. Moreover, an increase in para-diethylbenzene selectivity was observed. © 1998 Academic Press

Key Words: **zeolite H-ZSM-5; coke regeneration; ethylbenzene disproportionation; IR; NMR.**

INTRODUCTION

Deactivation of zeolite catalysts mainly results from the formation of carbonaceous residues, commonly known as "coke." It has been generally concluded (1–4) that the formation of carbonaceous deposits and their action upon the zeolites depends, not only on the characteristics of the zeolite catalyst, but also on the nature of the reactants involved and the related operating conditions. Extensive investigations have been made on coking and deactivation of zeolites (5–12) and the subject has been comprehensively reviewed (1–4). The activity of the fouled zeolite catalyst can be regenerated by the combustion of coke at an elevated temperature (13–14). Such oxidative treatment which is normally done under the flow of air or diluted oxygen depends on the characteristics of the coke and the thermal stability of the zeolite catalyst. As most of the work regarding the regeneration of the zeolites is done by industrial researchers, the results are sparingly available in the open literature.

Magnoux *et al.* (14) observed that the oxidation rate of the carbonaceous compounds formed during the *n*-heptane transformation is nearly independent of the coke content. The rate, however, strongly depends on the structure of the zeolites. Hence the authors concluded that, similar to coking and aging, coke oxidation is a shape-selective process. Using pyrene impregnated on the zeolite Y as a model reaction for characterizing the mechanism of the coke oxidation, Moljord *et al.* (15) concluded that three types of reactions may take place during coke oxidation: (i) condensation of polyaromatic molecules, (ii) oxidation of polyaromatics into aldehydes, ketones, acids, and anhydrides, and (iii) decarboxylation or decarbonylation of the oxygenated compounds. In a separate study, the same authors (16) further revealed that during propene transformation over H-Y zeolites, the oxidative removal of coke has a much stronger dependence on zeolite composition than the composition of coke. The coke residues were more easily oxidized in zeolites having a higher content of framework aluminum atoms. Bauer *et al.* (17) studied the effect of carrier gases (*viz*. hydrogen and alkanes) on the reactivation of coked H-ZSM-5 zeolite during methanol to hydrocarbon reaction. These carrier gases showed a lower deactivation rate than nitrogen. In addition, spent catalysts were partially reactivated by alkane treatment. The authors hence concluded that dissociative adsorption of hydrogen and alkanes on a few active sites are responsible for the hydrocracking of carbonaceous deposits.

The objective of this work is to study the reactivation of H-ZSM-5 zeolite that coked during ethylbenzene conversion. The transformation and successive removal of cokes during regeneration in the presence of air are examined. In addition, the reactivation performance of the coked zeolite sample in the presence of air, 0.5% O_2 in N_2 and H_2 at 500°C is compared. A possible mechanism for the reactivation of coked samples is proposed.

[1] Corresponding author.

0021-9517/98 $25.00

EXPERIMENTAL

Powdered, binderless H-ZSM-5 zeolite ($SiO_2/Al_2O_3 = 51$; Strem Chemicals, Inc.) was used whose structure and framework composition was confirmed by powder X-ray diffraction and ^{29}Si magic-angle-spinning (MAS) NMR. Ethylbenzene (A.R. grade) was obtained from Merck–Schuchardt and was used without further purification. All catalytic reactions and the reactivation of the coked sample were conducted in a continuous flow fixed-bed microreactor. Palletized catalyst sample (10–20 mesh) was used for all the reactions. The initial coked sample was obtained by carrying out ethylbenzene (EB) disproportionation reaction at 330°C at space velocity (WHSV) 0.52 h^{-1} and N_2/EB molar ratio 2 for 8 days. The purpose of using such long contact time is to promote high conversion and, hence, to ease the formation of coke (18). The total coke content of the parent coked sample so obtained was ca 14.5 wt%.

The coked samples were regenerated in the presence of air at 500°C for 0.2, 0.5, 1.0, 2.0, and 6.0 h. The activity of these partially regenerated samples were tested for EB disproportionation reaction carried out at 300°C with WHSV = 7.4 h^{-1} and N_2/EB = 2. The compositions of the reactor effluents were analyzed by gas chromatograph (Shimadzu GC-4A) using a packed column (5% SP-1200 and 1.75% Bentone 34 on 100/120 Suplecoport, 6 ft).

The coked sample was also reactivated in the presence air, 0.5% O_2 in N_2 and H_2 at 500°C until the samples give the same catalytic activity (about 10 wt% of the EB conversion). The catalytic activities of the reactivated samples were then respectively tested for ethylbenzene conversion under the condition: temperature 300°C; WHSV = 7.4 h^{-1}; N_2/EB = 2.

Thermogravimetric analyses (TGA) were conducted with a ULVAC TGD-7000RH thermogravimetric system. The TGA studies were carried out under different carrier gases, namely air, 0.5% O_2 in N_2, H_2, or N_2. Typically, the thermograms were recorded among 25–930°C while maintaining the carrier gas flow rate at 100 ml min^{-1} and a heating rate of 2°C min^{-1}. To determine the sample coke content, separate experiments were carried out using air as the carrier gas (heating rate 10°C min^{-1}). The coke content for each sample was then determined from the weight loss between 300 and 700°C. Prior to the TGA study, all fouled samples were stored over a saturated NaCl solution in a desiccator for at least 24 h. Diffuse reflectance infrared (IR) experiments were carried out using a Bruker IFS-28 FTIR spectrometer. The IR spectra were recorded *in situ* while the sample was subjected to regeneration in air at 500°C.

Prior to the ^{129}Xe NMR and xenon adsorption experiments each sample was first dehydrated by gradual heating to 200°C under vacuum ($<10^{-5}$ Torr, 1 Torr = 133.32 Pa) and was then maintained at the same temperature for at least 18 h. The sample tube configuration was designed so that a standard 10-mm NMR tube joined to a vacuum stopcock could be conveniently set up for thermal treatment as well as adsorption of xenon on a vacuum setup. Adsorption experiments were done at room temperature (25°C) using a volumetric method (18). ^{129}Xe NMR spectra were recorded on a Bruker MSL-300P NMR spectrometer operating at a resonance frequency 83.012 MHz. Typically, 200–2000 free induction decay (FID) signals were accumulated with a relaxation delay 0.3 s. The ^{129}Xe NMR chemical shift was referred to that of diluted xenon gas. ^{13}C CP-MAS NMR experiments were performed on a Bruker MSL-500P spectrometer with a resonance frequency of 125.77 MHz. The spinning frequency of the rotor was kept at 8 kHz. Depending upon the amount of coke present, typically ca 30,000–40,000 FID signals were accumulated using a recycle delay of 1.0 s (18, 19).

RESULTS AND DISCUSSION

Catalyst Regeneration in Air

(a) Duration of regeneration. The effect of duration of regeneration (hereafter denoted by τ_r) was studied by reactivation of the sample in the presence of air at 500°C for 0.2, 0.5, 1.0, 2.0, and 6.0 h, respectively. The regenerated samples taken at these specific periods were subjected to thermogravimetric analysis and EB conversion test reaction (*vide supra*) separately. The latter experiment was carried out so that the residual activity and the catalytic performance of the fouled samples can be readily followed (Table 1). The results reveal that the coked catalyst yielded a significantly higher fraction of *para*-diethylbenzene (*p*-DEB) among all the DEB isomers. This is possibly a result of coke-induced

TABLE 1

Product Distribution of Air-Regenerated H-ZSM-5 Catalysts during Ethylbenzene Disproportionation

Regeneration time (h)	Parent cat.	0	0.2	0.5	1	6
Coke content (±0.1 wt%)[a]	0	14.5	11.2	4.5	3.0	0
Conversion (wt%)[b]	14.5	2.0	6.7	10.7	12.2	14.3
Selectivity						
p-diethylbenzene	18.8	35.2	19.9	20.0	20.0	19.7
m-diethylbenzene	39.3	25.7	40.9	41.5	41.0	41.3
o-diethylbenzene	1.3	0	1.4	1.8	1.2	1.8
benzene	30.8	32.4	31.3	32.2	32.8	32.1
toluene	0.4	0	0.3	0.3	0.4	0.4
xylene	2.1	3.3	3.0	2.7	2.4	2.3
others	7.5	3.4	3.1	1.5	2.2	2.5
p-diEB/diEB (%)	31.7	57.8	32.0	31.7	32.2	31.9

[a] Obtained from TGA.
[b] Time-on-stream: 2 h.

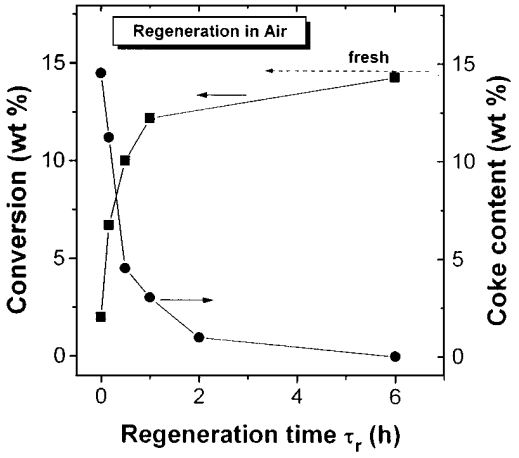

FIG. 1. The variations of ethylbenzene conversion and coke content with duration of regeneration in the presence of air.

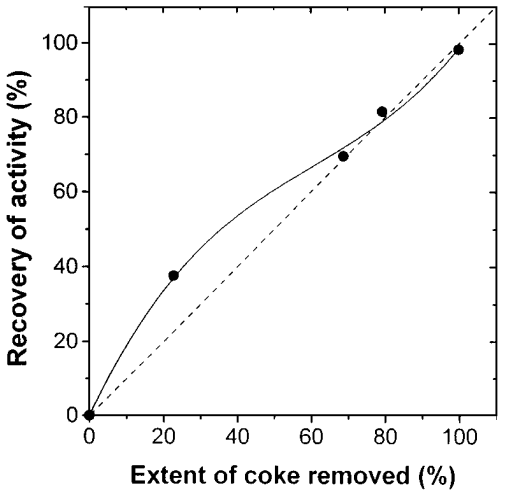

FIG. 2. Fractional variations of the activity recovered with the extent of coke removed during air-regenerated process.

shape selectivity in the H-ZSM-5 zeolite (20). However, upon immediate regeneration of the coked sample by oxidative removal, the *p-/m*-DEB ratio among the DEB isomers becomes constant and appeared to be close to that expected for an equilibrium composition. Moreover, it is noted that the fraction of benzene produced over all regenerated samples remained nearly constant. It will be shown later that the variation in the product selectivity is closely related to the deposition and removal of internal and external cokes.

The variations of the conversion and total coke content as a function of regeneration time is depicted in Fig. 1. A rapid increase in the rate of reactivation was observed during the first 0.5 h, ca 67% of the total coke was removed. At $\tau_r = 2$ h, over 93 wt% of the coke was removed. A complete removal of coke was reached at $\tau_r = 6$ h. The removal of coke is therefore most effective during the initial regeneration ($\tau_r < 1$ h) and, hence, resulted in a sharp increase in conversion. Similarly, it was found that coking is responsible for catalyst deactivation and that the effect is more pronounced at the initial stage of the EB disproportionation reaction due to the shielding of strong acid sites by coke formation (18). The above results therefore indicate that the effectiveness of regeneration (and, hence, the conversion level or the rate of reactivation) is closely related to the duration of regeneration (and hence the amount of residual coke content). Although the most effective regeneration occurs during the initial stage, a nonlinear relation exists between the observed activity regained and the coke removed, as showed in Fig. 2. For example, at $\tau_r = 0.2$ h, ca 38% of the original activity was regained while 23% of coke have been removed; whereas, at $\tau_r = 1$ h, 79% of the coke removal corresponds to 82% of regained activity.

Figure 3 shows the xenon adsorption isotherms of the fresh, coked, and partially regenerated samples. Relative adsorption capacity generated by oxidative removal of the coke can be obtained from the adsorption isotherm. The initial coked sample without regeneration treatment has the least amount of adsorption, as expected. The increase in adsorption capacity with increasing regeneration time therefore corresponds to a successive removal of coke. It may be noted that after $\tau_r = 0.2$ h, corresponding to coke removal of ca 23%, but more than 1/3 of the adsorption capacity of the parent H-ZSM-5 zeolite sample was regained. Hence, the results indicate that intracrystalline coke present in the zeolite is preferentially removed at the early regeneration stage.

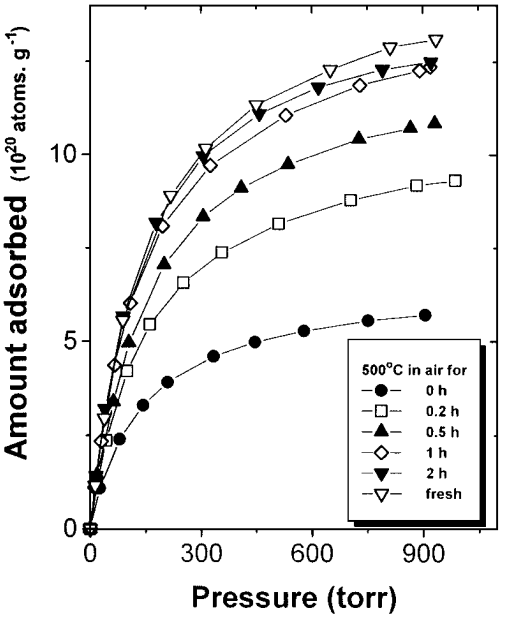

FIG. 3. Xenon adsorption isotherms of fresh and coked H-ZSM-5 zeolite regenerated in air at 500°C for varied duration of time.

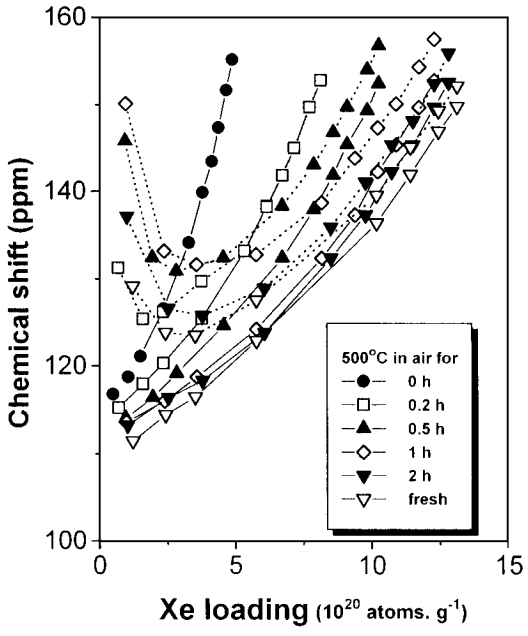

FIG. 4. The variations of ^{129}Xe NMR chemical shifts with xenon loading for fresh and coked H-ZSM-5 zeolite regenerated in air at 500°C for varied duration of time.

^{129}Xe NMR is a unique technique that can provide information about the location of the coke present in the zeolite catalysts (18, 19, 21). Figure 4 displays the variation of ^{129}Xe chemical shifts $\delta(\rho)$, with xenon density ρ, for the fresh H-ZSM-5, as well as the coked and partially reactivated samples. The chemical shift profiles for the fresh and partially coked samples all show two ^{129}Xe NMR lines similar to the previous observations (18). The signals appearing at higher chemical shift are predominant only at low xenon density. These signals that resulted in a concave chemical shift curve at low xenon loading can be ascribed to the presence of strong adsorption sites in the zeolite channels, such as solid state defects or extra-framework aluminum, in the zeolite channels (22, 23). As these signals are not characteristic of the zeolite channels itself, they were not considered in estimating ^{129}Xe NMR parameters. The slope of the (lower) chemical shift curve at high xenon loading, σ_{xe}, reflects the effect of binary collisions between two xenon atoms (24–26); its variation can be correlated to the change in free volume of the catalyst upon coking. The relative change in the free volume can be expressed (24) as

$$V/V_0 = (\sigma_{xe})_{fresh}/(\sigma_{xe})_{coked}, \qquad [1]$$

where V is the internal volume of the coked sample and V_0 is the internal volume of the uncoked (fresh) sample.

The variations of σ_{xe} and V/V_0 with coke content are presented in Fig. 5. In this context, a decrease in the coke content reflects an increase in regeneration time. It is also noted that, before the regeneration, the effective free volume of the coked sample is only ca 35% of the parent (fresh) H-ZSM-5 zeolite. As revealed by Fig. 5, during the initial stage of regeneration ($\tau_r \leq 0.5$ h; i.e., coke content decrease from ca 14.5 to ca 5.0 wt%) there is a steep decrease in the value of σ_{xe}, whereas at a later stage ($\tau_r \geq 0.5$ h; coke content decreases from 5.0 to 0 wt%) the variation in σ_{xe} is much less. Correspondingly, increasing regeneration time (or decrease in coke content) resulted in a sharp increase in the volume of the zeolite at the early stages and a less appreciable increase at the later stage. The above results show that coke molecules present in the intracrystalline zeolite channels are preferably removed during the early stages of regeneration. The results are in accord with the previous results obtained from the Xe adsorption data. Those cokes which deposit on the outer surface of the zeolite crystallites merely contribute to the total effective free volume of the catalyst upon regeneration and are removed less efficiently. Bibby *et al.* (12) found that oxygen plasma is fairly effective in removing cokes, particularly the external cokes. We note that the present results go further to clarify that, during the early stage of regeneration, internal cokes are preferentially removed.

(b) Nature of coke. The ^{13}C CP-MAS NMR spectra of the coked H-ZSM-5 sample before and after successive regeneration are presented in Fig. 6. All the spectra exhibit broad features in the 110–160 ppm region, which are assigned to the aromatic carbons. While prior to regeneration, the coked zeolite sample also reveals presence of resonance peaks in the 0–40 ppm region, which are ascribed to aliphatic carbons. The lines of aromatic species correspond (27, 28) to the presence of nonsubstituted aromatic carbons (120–130 ppm), carbon bridges between aromatic rings (130–140 ppm), and substituted aromatic

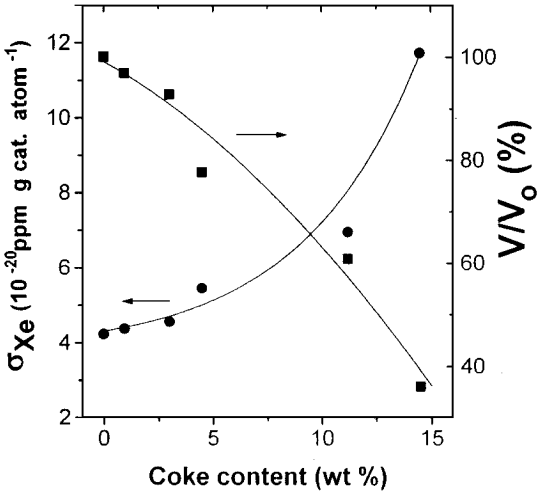

FIG. 5. Plot of σ_{xe} and the corresponding V/V_0 (see text) as a function of coke content for coked H-ZSM-5 catalyst with varied extent of reactivation in air. The data for zero coke content were taken from the fresh catalyst.

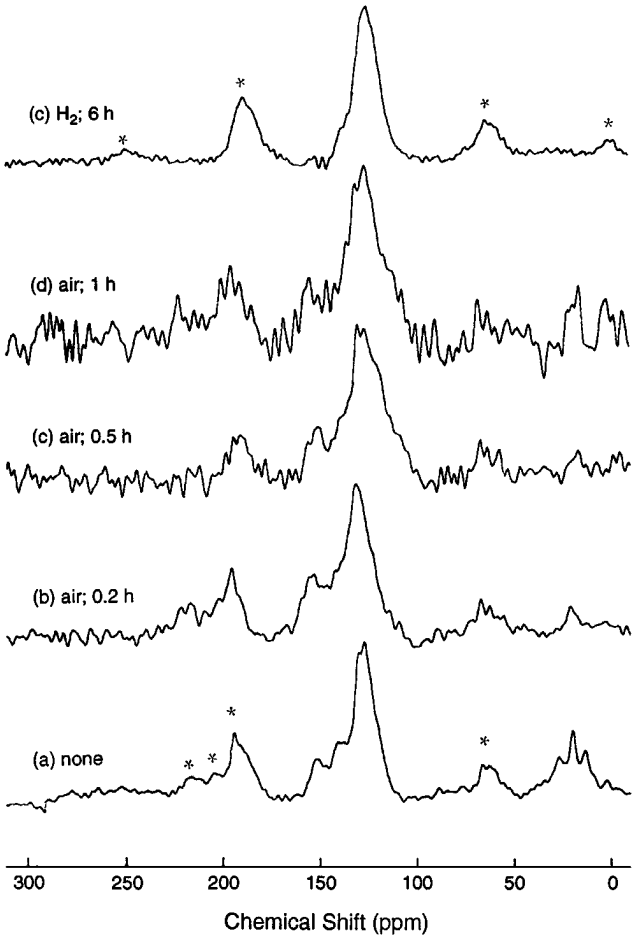

FIG. 6. The ^{13}C CP-MAS NMR spectra of (a) coked H-ZSM-5 zeolite sample regenerated at 500°C (b)–(d) in air for $\tau_r = 0.2$, 0.5, and 1.0 h, respectively, and (e) in H_2 for 6 h. The peaks denoted by an asterisk represent spinning side-bands.

carbons (140–150 ppm). Besides these aromatic signals, spectra in Figs. 6a–6d all reveal a shoulder peak at 153 ppm which may be ascribed to the substituted aromatic carbon to which either hydroxy, alkoxy group is attached (27, 28). It has been shown (29) that alcohols may be formed after the exposure of the coked zeolite sample to the atmospheric moisture. Novakova *et al.* (30) also noticed the presence of such resonance peak at 154 ppm in the H-ZSM-5 sample fouled during acetone conversion. The authors ascribed the resonance peak to the presence of aromatic ethers. Since we did not observe any resonance near 50–80 ppm, even upon variation of spinning rate, thus the existence of an alkoxy group is highly unlikely. Hence, the presence of aromatic ethers may be ruled out. The peak located at 153 ppm can be, a priori, ascribed to the aromatic hydroxy species which exist as intracrystalline coke residues.

Moreover, the absence of the aliphatic resonance in the spectra of the partially regenerated samples (Figs. 6b–6d) indicates that the process probably begins with the oxidation of alkyl groups attached to the aromatic rings. The broadening of the aromatic peak and the decrease in signal sensitivity upon successive regeneration also indicate the possible formation of highly condensed polyaromatic compounds (19, 31) during the processes. Such condensed polyaromatic compounds were also observed (15) during oxidation of pyrene on zeolite Y.

The IR spectra of the coked and partially regenerated samples are depicted in Fig. 7. The absorption peak at 3600 cm^{-1} is assigned (32, 33) to hydroxyl vibration (O–H stretching) bands of the Brønsted acid sites, whereas the absorption at 3740 cm^{-1} is assigned to the nonacidic silanol groups which may be present on the crystalline defect sites or external surfaces. For the coked H-ZSM-5 sample (Fig. 7a), additional weak absorption bands in the 2800–3100 cm^{-1} region were found. These bands are ascribed to the C–H vibrational modes of the carbonaceous compounds. More specifically, bands between 2800–3000 cm^{-1} can be ascribed to the presence of aliphatics, whereas those in the range 3000–3200 cm^{-1} can be ascribed to aromatics of carbonaceous compounds. It is noted that the aliphatic bands disappear after 0.2 h of regeneration. Hence, similar to the ^{13}C CP-MAS NMR results, the IR results also indicate that the oxidation of coke molecules begins with the alkyl groups which are attached to the polyaromatic rings. It was also observed that the band for the C–H stretching vibration mode of the aromatics is shifted towards higher frequency during the course of regeneration (Fig. 7b–7e). The latter is most probably due to the formation of condensed

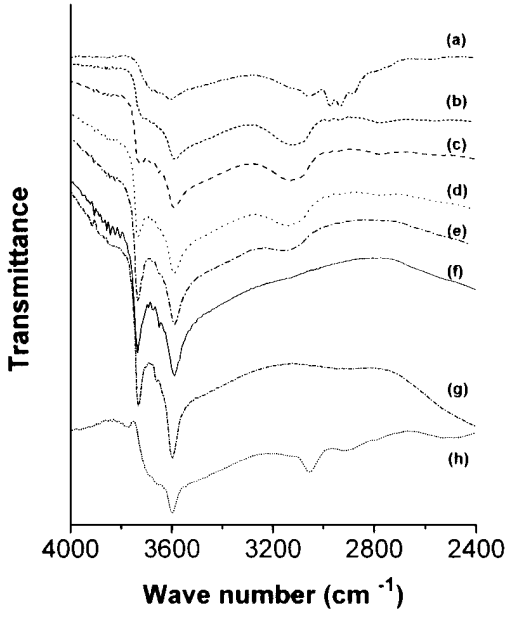

FIG. 7. IR spectra of the (a) coked H-ZSM-5 zeolite, (b)–(f) coked H-ZSM-5 zeolite sample regenerated in air with $\tau_r = 0.2$, 0.5, 1.0, 2.0, and 6.0, respectively, compared to (g) fresh H-ZSM-5 zeolite and (h) coked H-ZSM-5 zeolite sample regenerated in H_2 with $\tau_r = 6.0$ h.

polyaromatic compounds. These compounds get completely oxidized upon further regeneration (Fig. 7f).

Another notable difference in these spectra is the absorbance of the band at 3600 cm^{-1} increases with τ_r and the integrated area of this band becomes almost equal to that of the fresh zeolite sample after $\tau_r > 1$ h. In contrast to this observation, an appreciable increase in the intensity of the 3740 cm^{-1} band is noticeable only after $\tau_r > 1$ h. Hence, it may be concluded that, during regeneration, the cokes present near the Brønsted acid sites are removed preferentially, whereas the cokes present on the extracrystalline surfaces or defect sites require more time for the oxidative removal. Since most of the acid sites are located inside the channels in the crystallites, preferential removal of the internal coke can be explained. Removal of the internal coke, especially for those located near the acid sites, would also account for the rapid initial increase in the EB conversion and the variation of product selectivity with the coke removal. By the same token, the gain of more than 1/3 of the xenon adsorption capacity with only ca 23% removal of the coke (Fig. 3) and variation of σ_{xe} (Fig. 5) can also be explained by the preferential removal of the internal coke during the early stage of regeneration.

Guisnet and co-workers (16) have suggested that for fouled HY zeolites coke removal by oxidation treatment invokes active participation of acid sites. Using electron microscopy and electron energy loss spectroscopy (EELS), the same group (34, 35) concluded that cokes formed on the external surface of H-ZSM-5 zeolite crystallites during *n*-heptane cracking are similar to that of coronene (bulky polyaromatic-pregraphitic), whereas those formed in the intracrystalline channels exhibit a low polyaromatic character. These observations, together with the present findings suggest that the bulky polyaromatic nature and deficiency of external acid sites make the oxidative removal of the external cokes more difficult.

Next, let us discuss the possible mechanism for the coke selectivation process. In this context, a notable increase in *para*-selectivity was found in the reaction on the parent coked sample (before regeneration). However, when the coked sample was subjected to oxidation treatment, the selectivity seemingly decreases close to its thermal equilibrium value. It is generally accepted that the enhancement of *para*-selectivity during important reactions on zeolites, such as alkylation, isomerization, transalkylation, and disproportionation of monoalkylbenzenes, is mainly due to two debating mechanisms that require catalyst surface modification (36–41), namely the diffusional constraint provoked by the decrease in pore-opening and the inactivation of acid sites on the external surfaces.

It is worth noting that the effect of surface modification on product selectivity should also be a strong dependent of the morphology, crystalline size, and acidity (or Si/Al ratio) of the zeolite (42–44). Consequently, the two possible mechanisms described above are still in debate. For example, several reports (36, 37) have revealed that the enhancement of *para*-selectivity during methylation of toluene over H-ZSM-5 zeolites was ascribable more closely to the narrowing of pore-opening rather than to the site blocking by external cokes. On the other hand, it is also reported that the deposition of external cokes effectively modifies the surface acid properties of the zeolite crystallites that, in turn, cut off the secondary isomerization pathways (39, 40) of the product isomers and thus enhance the *para*-selectivity. Moreover, in a more recent work, Fang *et al.* (41) demonstrated that the threshold for such *para*-selectivity enhancement is very sensitive to the *complete* retardation of external acid sites by coke formation. Such coke-induced selectivity may break down during sample regeneration even by partial reactivation of external acid sites.

In the present work, the observed *para*-selectivity in the parent coked sample (before regeneration) can be explained by the retardation of the external acid sites by coking. Similarly, the selectivity change during the early stage of the regeneration can be explained by the partial reactivation of external acid sites. However, the possibility of *para*-selectivity enhancement provoked by diffusional constraints due to narrowing of pore-opening by coking cannot be completely ruled out. The detailed mechanism for the coke-induced product selectivity during catalytic reactions over zeolites demands further investigation. In fact, a portion of this important issue has been studied in a separate collaborative work of this laboratory (41).

Catalyst Regeneration in Other Gases

(a) Location of coke. The effects of reactivation of coked zeolite catalyst were also examined using different reactivating gases, namely air, 0.5% O_2 in pure nitrogen, and H_2. Before the reactivation, the conversion for the coked H-ZSM-5 zeolite is ca 2.0 wt% and with *p*-DEB ca 57.8% (Table 2). For easy comparison, samples reactivated to a different extent were kept at about the same activity (ca 10 wt% EB conversion) during the test reaction (*vide supra*). It is interesting that although the activity of these samples upon reactivation is almost the same, but the amount of coke present in these samples evidently varies with the regeneration conditions (Table 2). The least amount of coke (2.5 wt%) was observed for sample reactivated in 0.5% O_2 in N_2; however the process required $\tau_r \geq 20$ h. In the presence of air (i.e., 21% O_2 in N_2), the reactivation can be carried out within 0.5 h and the amount of coke present in the partially reactivated sample was 4.5 wt%. In the presence of H_2, the same activity of the catalyst can be obtained after 6 h, but 9.0 wt% of the coke is still present in the sample. The product distributions during EB conversion over these samples were observed to be about the same; samples reactivated in the presence of air

TABLE 2

Product Distribution of Regenerated H-ZSM-5 during Ethylbenzene Disproportionation

Regenerating gas	None	Air	0.5% O_2/N_2	H_2
Reg. time τ_r (h)	0	0.5	20	6
Coke content (±0.1 wt%)[a]	14.5	4.5	2.5	9.0
Conversion (wt%)[b]	2.0	10.7	10.3	9.6
Selectivity				
p-diethylbenzene	35.2	20.0	20.4	21.6
m-diethylbenzene	25.7	41.5	41.9	40.0
o-diethylbenzene	0	1.8	1.4	0.3
benzene	32.4	32.2	30.8	31.9
toluene	0	0.3	0.3	0.2
xylene	3.3	2.7	3.1	3.3
others	3.4	1.5	2.2	2.6
p-diEB/diEB (%)	57.8	32.0	32.0	34.9

[a] Obtained from TGA.
[b] Time-on-stream: 2 h.

and diluted O_2 gave equilibrium composition of the diEB isomers, while formation of *p*-DEB was a little more when H_2 was used. The increase in the *para*-selectivity may be due to the relatively more amount of external cokes present.

Figure 8 represents the xenon adsorption isotherms of the fresh and the coked samples which were reactivated in the presence of various gases to the same extent. The observed adsorption capacities of the reactivated samples are almost the same, irrespective of the marked difference in

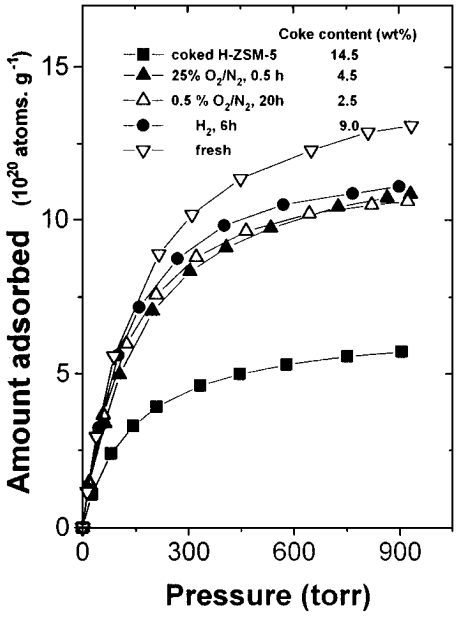

FIG. 8. Xenon adsorption isotherms of the coked H-ZSM-5 zeolite regenerated in air, 0.5% O_2 in N_2, and in H_2 compared to that of the fresh and original coked samples.

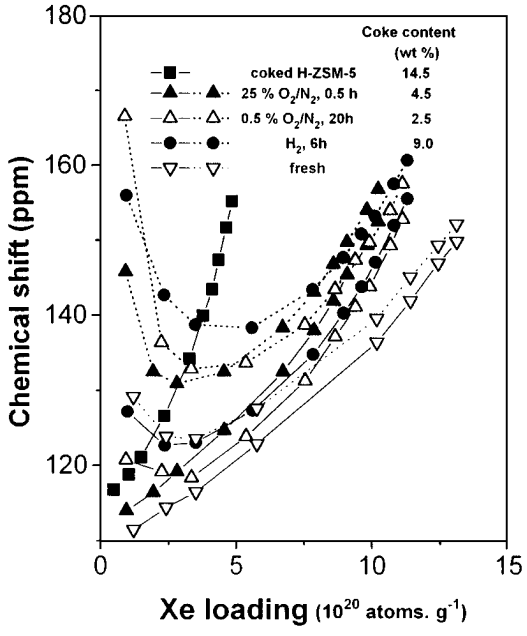

FIG. 9. The variations of ^{129}Xe NMR chemical shifts with xenon loading for the coked H-ZSM-5 zeolite regenerated in air, 0.5% O_2 in N_2, and in H_2 compared to that of the fresh and original coked samples.

their total coke content (Table 2). Figure 9 displays the variations of ^{129}Xe NMR chemical shifts with xenon density of the reactivated samples in presence of various gases. Similar to the results of regeneration in air (Fig. 4), two ^{129}Xe NMR signals were observed at low xenon density when the coked catalysts were regenerated in the presence of diluted O_2 and H_2. Again, the curves appearing at higher chemical shifts were not considered in this context while estimating the NMR parameters (*vide supra*). The slopes of the curves of the coked samples reactivated in the presence of air, 0.5% O_2 in N_2, and H_2 are 5.5, 5.1, and 5.2 ($\times 10^{-20}$ ppm · g cat · atom^{-1}), respectively. According to Eq. [1], these values therefore indicate that the effective free volumes of the reactivated samples are about the same, irrespective of the various amounts of coke present in the zeolite.

For catalysts regenerated in the presence of H_2, while the total free volume recovered is ca 80% of the fresh catalyst, only ca 38% (5.5 wt%) of the coke was removed. The result indicates that, while using H_2 as the regenerating gas, more intracrystalline coke is preferentially removed than coke deposited on the extracrystalline surfaces. By the same token, when using air or diluted O_2 as the regenerating gas, while about the same amount of total free volume was recovered (Fig. 8), ca 69% (air; 10 wt%) and 83% (diluted O_2; 12 wt%) were removed, respectively. In the latter two cases, intracrystalline and extracrystalline coke seems to be removed simultaneously.

(b) Nature of coke. The thermograms of sample in the presence of different reactivating gases are presented in Fig. 10. As shown in the figure, the weight loss for $T < 250°C$

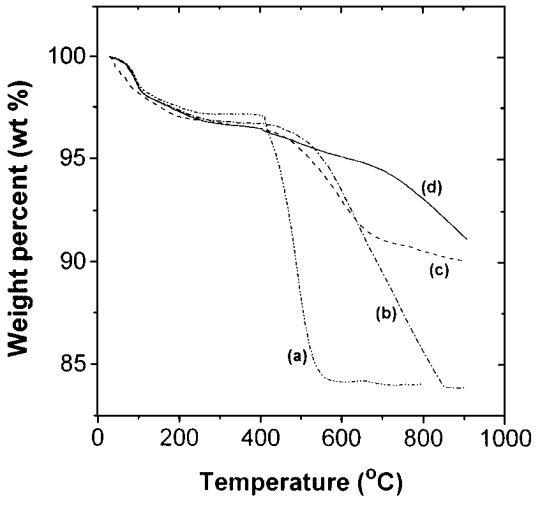

FIG. 10. Comparison of the thermograms of the coked H-ZSM-5 zeolite regenerated in (a) air, (b) 0.5% O_2 in N_2, (c) H_2, and (d) N_2.

can be ascribed to the loss of water and residual liquid reactants. Another notable weight loss in thermograms begins at $T = 410°C$ for all samples. In the cases using N_2 and H_2 as regenerating gases, two apparent regions of weight loss were observed at $T > 410°C$ due to the cracking of coke molecules; the weight loss at the lower temperature region may arise from dissociation of alkyl species from the aromatics, whereas that at the higher temperature is due to the loss of bulky polyaromatic cokes. The amount of weight loss is more pronounced in the presence of H_2 than N_2 indicates that the former is more efficient in coke removal. In both cases, however, cokes cannot be completely removed even at temperatures as high as 900°C. Moreover, for regeneration in the presence of diluted O_2, almost all the cokes can be oxidized at 880°C when the sample was reactivated in 0.5% O_2 in N_2; the maximum rate of weight loss is ca 690°C. While reactivating in air, a complete coke oxidation occurred at a much lower temperature (550°C) with the maximum rate of weight loss at ca 490°C. Thus, it may be concluded that the combustion of lightweight molecules produced from the cracking reaction is responsible for the initiation of the coke oxidation.

The ^{13}C CP-MAS NMR spectra of the samples reactivated in the presence of air is illustrated in Figs. 6b–6d, whereas that reactivated in H_2 is shown in Fig. 6e for comparison. Apparently, the resonance peaks at ca 144 and 153 ppm are absent for the sample reactivated in H_2. This might be due to hydrocracking of alkyl and hydroxy groups attached to the condensed aromatics and, thus forming the lightweight polynuclear aromatic compounds. The above results support the previous speculation that the peak appearing at 153 ppm is due to phenolic compounds which are effectively removed in the presence of H_2. Bauer *et al.* (17) proposed that the reactivation of coked H-ZSM-5 may take place through dissociative adsorption of H_2 on sites which facilitate the hydrocracking of coke molecules.

The IR spectra of the sample partially reactivated in the presence of H_2 is also shown in Fig. 7h. By comparing to the coked H-ZSM-5 zeolite sample (Fig. 7a), clearly the band at 3600 cm^{-1} has gained intensity upon reactivation in H_2. As this band is associated with the Brønsted acid sites, partial reactivation of the coked samples can be explained. It is very noteworthy that after the reactivation in H_2, the band at 3740 cm^{-1} (nonacidic silanol group) is absent, in contrast to the spectra obtained from the air-reactivated samples (Figs. 7b–7f). The above observation therefore indicates that, while regenerating with H_2, the cokes formed at the external surface or defect sites are not removed, whereas in the presence of O_2, both intra- and extra-crystalline cokes are oxidized. Moreover, it is noted that the C–H vibrational band of aliphatics (2800–3000 cm^{-1}) is absent after reactivation of the coked sample in the presence of hydrogen. However, the C–H vibrational band of aromatics (3000–3200 cm^{-1}) remains unaltered during the reactivation. Hence, the IR results further support the previous speculation that hydrocracking of alkyl groups which attached to condensed aromatic rings may take place during reactivation of coked zeolite sample.

The above adsorption, IR and NMR results therefore indicate that the internal coke was removed more efficiently under H_2 environment. Since most of the acid sites are located inside the crystallites, the internal cokes therefore were removed by acid site-assisted hydrocracking processes. On the other hand, for the external cokes, alkyl-substituted groups are more likely to be removed.

CONCLUSIONS

During the initial coke regeneration in air or diluted O_2, coke present in the intracrystalline channels is removed preferentially to that present on the external surface. The rate of regeneration is much higher at the initial stages of the regeneration. Reactivating gases used during regeneration have a great influence on selective removal of the coke. During oxidative removal of the coke in the presence of air or diluted O_2, alkyl polyaromatic carbonaceous compounds become converted into a more condensed structure during coke oxidation. Although coke present in the intracrystalline channels is removed during the oxidation, some coke present on the external surface of the crystallites is also removed. The activity of the catalyst can also be partly recovered while the coked catalyst is reactivated in the presence of H_2, although a lesser amount of coke is removed in this case. Partial hydrocracking of bulky alkyl polynuclear aromatic compounds present on the external surfaces may take place during activation. This results in the formation of less bulky polyaromatic compounds. Moreover, while regenerated in H_2, most of the intracrystalline

coke was removed by hydrocracking reactions. The results also indicate that Brønsted acid sites play an important role during regeneration.

ACKNOWLEDGMENTS

The support of this work from the National Science Council of Republic of China (NSC86-2113-M001-005) is gratefully acknowledged. S.J.J. is a postdoctoral fellow of Academia Sinica.

REFERENCES

1. Guisnet, M., and Magnoux, P., *Appl. Catal.* **54**, 1 (1989).
2. Bhatia, S., Beltramini, J., and Do, D. D., *Catal. Rev.-Sci. Eng.* **31**, 431 (1989–1990).
3. Karge, H. G., *Stud. Surf. Sci. Catal.* **58**, 531 (1991).
4. Bibby, D. M., Howe, R. F., and McLellan, G. D., *Appl. Catal. A* **93**, 1 (1992).
5. Derouane, E. G., and Gabelica, Z., *J. Catal.* **65**, 486 (1980).
6. Olson, D. H., and Haag, W. O., *ACS Sympos. Ser.* **248**, 275 (1984).
7. Rollman, L. D., and Walsh, D. E., *J. Catal.* **56**, 139 (1979).
8. Rollman, L. D, *J. Catal.* **47**, 113 (1977).
9. Chen, N. Y., and Garwood, W. E., *Catal. Rev.-Sci. Eng.* **28**, 185 (1986).
10. Magnoux, P., Cartraud, P., Mignard, S., and Guisnet, M., *J. Catal.* **106**, 242 (1987).
11. Wojciechowski, B. W., and Corma, A., "Catalytic Cracking." Dekker, New York (1986).
12. Bibby, D. M., Milestone, N. B., Patternson, J. E., and Aldridge, L. P., *J. Catal.* **97**, 493 (1986).
13. Penick, J. E., Lee, W., and Maziuk, J., *ACS Sympos. Ser.* **266**, 18 (1987).
14. Magnoux, P., and Guisnet, M., *Appl. Catal.* **38**, 341 (1988).
15. Moljord, K., Magnoux, P., and Guisnet, M., *Catal. Lett.* **28**, 53 (1994).
16. Moljord, K., Magnoux, P., and Guisnet, M., *Catal. Lett.* **25**, 141 (1994).
17. Bauer, F., Ernst, H., Geidel, E., and Scodel, R., *J. Catal.* **164**, 146 (1996).
18. Chen, W. H., Jong, S. J., Pradhan, A. R., Lee, T. Y., Wang, I., Tsai, T. C., and Liu, S. B., *J. Chin. Chem. Soc.* **43**, 305 (1996).
19. Chen, W. H., Pradhan, A. R., Jong, S. J., Lee, T. Y., Wang, I., Tsai, T. C., and Liu, S. B., *J. Catal.* **163**, 436 (1996).
20. Chen, N. Y., Grawood, W. E., and Dwyer, F. G., "Shape Selectivity Catalysis in Industrial Applications." Dekker, New York, 1989. [*Chem. Ind. Ser.*, Vol. 36]
21. Bonardet, J. L., Barrage, M. C., and Fraissard, J., *J. Mol. Catal. A* **96**, 123 (1995).
22. Chen, Q. J., Guth, J. L., Seive, A., Caullet, P., and Fraissard, J., *Zeolites* **11**, 798 (1991).
23. Ryoo, R., Ihee, H., Kwak, J. H., Seo, G., and Liu, S. B., *Microporous Mater.* **4**, 59 (1995).
24. Fraissard, J. and Ito, T., *Zeolites* **8**, 350 (1988).
25. Demarquay, J., and Fraissard, J. P., *Chem. Phys. Lett.* **136**, 314 (1987).
26. Ito, T., Bonardet, J. L., Fraissard, J. P., Nagy, J. B., Andre, C., Gabelica, Z., and Derouane, E. G., *Appl. Catal.* **43**, L5 (1988).
27. Stothers, J. B., "Carbon-13 NMR Spectroscopy," p. 90. Academic Press, New York, 1972.
28. Silverstein, R. M., Basslers, G. C., and Morrill, T. C., "Spectroscopic Investigation of Organic Compounds," Chap. 5. Wiley, New York, 1991.
29. Haw, J. F., Richardson, B. R., Oshiro, I. S., Lazo, N. D., and Speed, J. A., *J. Am. Chem. Soc.* **111**, 2052 (1989).
30. Novakova, J., Kubelkova, L., Bosacek, V., and Mach, K., *Zeolites* **11**, 135 (1991).
31. Liu, S. B., Prasad, S., Wu, J. F., Ma, L. J., Yang, T. C., Chiou, J. T., Chang, J. Y., and Tsai, T. C., *J. Catal.* **142**, 664 (1993).
32. Auroux, A., Bolis, V., Wierzchowski, P., Gravelle, P. C., and Védrine, J. C., *J. Chem. Soc. Faraday Trans. I* **75**, 2544 (1979).
33. Védrine, J. C., Auroux, A., Bolis, V., Dejaifve, P., Nacache, C., Wierzchowski, P., Derouane, E. G., Nagy, J. B., Gilson, J. P., Van Hooff, J. H. C., Van de Berg, J. P., and Wolthuizen, J., *J. Catal.* **59**, 248 (1979).
34. Gallezot, P., Leclercq, C., Guisnet, M., and Magnoux, P., *J. Catal.* **114**, 100 (1988).
35. Magnoux, P., Cartraud, P., Mignard, S., and Guisnet, M., *J. Catal.* **106**, 242 (1987).
36. Čejka, J., Žilková, N., Wichterlová, B., Eder-Mirth, G., and Lercher, J. A., *Zeolites* **17**, 265 (1996).
37. Kim, J.-O., Ishida, A., Okajima, M., and Niwa, M., *J. Catal.* **161**, 387 (1996).
38. Wang, I., Ay, C. L., Lee, B. J., and Chen, M. H., *Appl. Catal.* **54**, 257 (1989).
39. Paparatto, G., Moretti, E., Leofanti, G., and Gatti, F., *J. Catal.* **105**, 227 (1987).
40. Lonyi, F., Engelhardt, J., and Kallo, D., *Zeolites* **11**, 169 (1991).
41. Fang, L. Y., Liu, S. B., and Wang, I., *Appl. Catal., A*, to be published.
42. Kaeding, W. W., *J. Catal.* **95**, 512 (1985).
43. Melson, S., and Schüth, F., *J. Catal.* **170**, 46 (1997).
44. Bhat, Y. S., Das, J., Rao, K. V., and Halgeri, A. B., *J. Catal.* **159**, 368 (1996).